Forensic Imaging 37 (2024) 200593

Contents lists available at ScienceDirect

Forensic Imaging

journal homepage: www.sciencedirect.com/journal/forensic-imaging

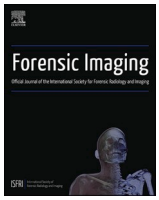

Development of a technique for postmortem CT angiography of fetuses with a lipophilic contrast agent

Jessica Vanhaebost [a,b,*], Nicolas Michoux [c], Xavier de Spiegeleire [c], Silke Grabherr [d,e,f], Emmanuel Coche [c]

[a] Department of Pathology and Legal Medicine, Belgium, Université Catholique de Louvain (UCLouvain) – Cliniques Universitaires Saint Luc, Brussels, Belgium
[b] Pole of Morphology, Faculty of Medicine, Institute of Experimental and Clinical Research, Université Catholique de Louvain, B-1200 Brussels, Belgium
[c] Institut du Cancer Roi Albert II (IRA2) - Institut de Recherche Expérimentale & Clinique (IREC) – Department of Radiology and Medical Imaging (IMAG), Université Catholique de Louvain (UCLouvain) – Cliniques Universitaires Saint Luc, Brussels, Belgium
[d] University Center of Legal Medicine Lausanne-Geneva, Chemin de la Vulliette 4, CH-1000, Lausanne 25, Switzerland
[e] Lausanne University Hospital, University of Lausanne, Lausanne, Switzerland
[f] Geneva University Hospital, University of Geneva, Geneva, Switzerland

ARTICLE INFO

Keywords:
Multidetector computed tomography
Lipophilic contrast agent
Vascular malformations
Fetopathology
Postmortem fetal CT angiography
Postmortem CT angiography

ABSTRACT

Background and objectives: Postmortem examinations of fetuses play a crucial role in confirming abnormalities, especially vascular and cardiac malformations leading to fetal demise. This study aims at developing and assessing a method for acquiring Post-Mortem CT-Angiography (PMCTA) with the injection of a lipophilic contrast agent (CA) to better visualize the great vessels of the trunk and head.
Materials and methods: 25 human fetuses (gestational age at death between 106 days and 28 weeks) were included. Examinations were performed using a dual-energy Multidetector Computed Tomography (MDCT) scanner. Three imaging sequences were acquired, before CA injection, after injection of 7mL of CA through umbilical artery (arterial phase), and after an injection of 15mL of CA through umbilical vein (venous phase). CA-induced vascular opacification was scored *per*-vessel in both phases as follows: 0 = none, 1 = partial, 2 = complete. Total opacification was defined as the sum of the *per*-vessel opacification scores.
Results: In 23/25 subjects, CA injection into the umbilical vessels was feasible manually using flexible catheters. After the first injection, at least a partial opacification of the arterial network was achieved in 15/23 (65%) subjects. After the second injection, a complete opacification of the venous network was achieved in 18/23 (78%) subjects. Failures occurred in 10/25 (40%) subjects and were mostly due to the preservation status.
Conclusion: PMCTA performed with a two-phase intra-umbilical injection of a lipophilic CA enabled to visualize the vascular network, even after a significant a postmortem interval. This protocol may help in detecting vascular malformations, improving clinical diagnoses and prenatal counselling.

Introduction

Fetopathology involves the examination of fetuses to identify abnormalities, particularly vascular or cardiac malformations that contribute to fetal death. The autopsy remains the gold-standard examination for evaluating the deaths of fetuses and stillborn children, after termination of pregnancy, miscarriage or unexpected intrauterine fetal death [1,2]. The addition of less invasive radiological examinations improve the results obtained during the autopsy by the pediatric pathologist and gives a better acceptance of the invasive procedure by the parents [3,4].

X-ray examination of stillbirths refines the results of the autopsy by allowing good visualization of the bone skeleton and by allowing better genetic guidance [5,6]. Whole body radiography remains an important diagnostic tool in adjunction to the fetal autopsy [7] but according to other studies, standard X-ray would not add diagnostic value to conventional autopsy of the fetus [8,9]. It is therefore difficult to justify the practice of routine post-mortem radiography in all cases of fetal

Abbreviations: CA, Contrast Agent; CRT, Cinematic Rendering Technique; MDCT, Multidetector computed tomography; MIP, Maximal Intensity Projection, MRI, Magnetic Resonance Imaging; NA, not assessable; PMCTA, Post-Mortem CT angiography; PMI, postmortem interval; VRT, Volume Rendering Technique.

* Corresponding author at Avenue Hippocrate 10, 1200 Brussels, Belgium.
E-mail address: jessica.vanhaebost@saintluc.uclouvain.be (J. Vanhaebost).

https://doi.org/10.1016/j.fri.2024.200593

Available online 20 April 2024

autopsies. However, it remains essential in cases of intrauterine growth retardation and syndromes involving skeletal abnormalities. Nevertheless, traditional autopsies for fetuses are often challenging due to the small size of most vessels, making dissection laborious or even impossible for some cases.

Postmortem ultrasound was developed because it is more available, even in developing countries, and it is cheaper [10]. The downsides of this method are that the cardiac anatomy is more difficult to evaluate and that artefacts resulting from the presence of air in the cardiac chambers are frequently encountered after feticide by intracardiac injections. In addition, there are operator-dependent artefacts.

Numerous studies [11–16] have demonstrated the benefit of post-mortem Magnetic Resonance Imaging (MRI) and have also compared it to conventional autopsy. MRI has been proposed as an alternative method of investigation to conventional autopsy in certain cases. This technique allows an accurate determination of congenital developmental malformations of the central nervous system, in particular in cases involving a limited contribution of autopsy analysis such as cases where advanced autolysis can be presumed. However, for fetuses with a gestational age < 20 weeks, MRI performance is poor [10].

MultiDetector Computed Tomography (MDCT) has also garnered attention for postmortem examinations due to its rapid acquisition, availability, and post-processing capabilities [11,17,18]. 3D images of human embryos (smaller specimens than fetuses) by combining solvent-based clearing methods were also proved effective to analyse nervous system development [19]. Diffusible iodine-based contrast-enhanced CT increase the soft-tissue visualization using a micro-CT but appears to be difficult in large fetuses, due to insufficient penetration of Lugol [19]. By injecting a contrast agent (CA) into the vascular system, the vascular lumen becomes visible, and organ parenchyma becomes contrasted, a technique known as Post-Mortem CT Angiography (PMCTA). This approach enables visualization of lethal malformations and provides answers to specific clinical queries raised by requesting clinicians [20–22].

While PMCTA in adults is well-established in the scientific literature [20,21,23–27], its application in pediatric cases, especially in fetuses, remains poorly explored, with only one study conducted on a porcine model [28]. A significant challenge encountered in PMCTA is that the contrast agent used in living patients cannot be utilized during the postmortem period due to extravasation through the vessel's porous wall resulting from postmortem alterations [29,30]. In 2015, Sarda–Quarello et al [31] described the feasibility and interest of performing perinatal postmortem angiography in order to provide additional information to prenatal investigations. More recently, Tumanova et al [32] demonstrated the importance of a radiological examination with angiography for a better diagnosis of vascular pathologies. This technique allows the separate study of arterial and venous vessels and makes it possible to identify both congenital anomalies of the heart and blood vessels, as well as their acquired pathologies in newborns. However, the method used was limited in time (no earlier than 12 h and no later than 48 h after the death of the newborn) due to the postmortem alterations undergone by the organs and tissues, more particularly the changes in the composition and properties of blood and the permeability, elasticity and integrity of vessels.

This study aims at assessing the efficiency of a CT acquisition protocol based on a postmortem injection of a lipophilic contrast agent to visualize the great vessels of the trunk and head. For this purpose, successes and failures in the procedure of injection were documented. Then the frequency of a vascular opacification score (defined as complete, partial or none) was assessed *per*-vessel and *per*-phase (arterial and venous). The presence of imaging artefacts and quality of the radiological examination were also assessed. Finally, the overall feasibility of the protocol and interpretability of images in routine clinical practice was discussed.

Materials and methods

Study population

This study was carried out in accordance with the declaration of Helsinki of the World Medical Association revised in 2013 for experiments involving humans for medical research purpose local and the protocol was approved by the local Ethics Committee. Anonymised specimens from the Department of Anatomy, donated for scientific research were included. The study prospectively included 25 human fetuses of gestational age at death between 106 days and 28 weeks (Table 1). The postmortem interval (PMI) varied between 5 days and 20 years and their weight varied between 39 g and 1498 g. Selection and exclusion criteria were established before the study: no previous autopsy performed on the fetus prior donation to the department of anatomy, stage of fetal development and residual length of the clamped umbilical cord. The gestational age of one fetus could not be determined because of its too small size and was noted NA (not assessable). Of the 25 fetuses examined, 21/25 (84 %) were frozen, 1/25 (4 %) was preserved in formalin and 3/25 (12%) were fresh (neither frozen nor preserved in formalin). Each fetus presented a state of more or less advanced postmortem alteration (e.g. skin maceration, gas throughout all anatomic spaces as the result of putrefaction, brain liquefaction).

Data collection

Each fetus was photographed and measured before the MDCT examination. Gestational age (in days) was assessed by obstetricians at the time of fetal death before donation to the anatomy department. The fetus was then measured, weighed, and its cranial perimeter measured, before the radiological examination. The length of the feet was also recorded. For each fetus, the interval between expulsion and examination was also recorded.

Imaging

Imaging examinations were performed on a dual-energy MDCT (Definition As Edge 128, Siemens™ Healthcare, Forcheim, Germany). The fetuses were placed on supine position. A scout-view (256 mm length) was first performed in order to determine the MDCT acquisition. Thereafter, unenhanced spiral acquisition was performed using the following parameters: 128 slices / rotation, collimation of 16 x 0.3 mm, reconstructed with a slice thickness of 0.4 mm, tube voltage: 80 kVp and a fixed tube current time product of 168mAs, field-of-view (FoV) depending of the size of the fetus. The kernel, a reconstruction algorithm used in computed tomography, was standard, and included smooth reconstruction kernel (U30) and sharp reconstruction kernel (U70). Three imaging sequences were performed during the same examination: before contrast agent injection (unenhanced MDCT), during the arterial phase (in order to better visualize the arterial opacification without superimposition with the venous network), and during the venous phase (after the vascular opacification) [33].

Injection of the contrast agent

Once unenhanced MDCT images were acquired, a 10 mL syringe was filled with a contrast medium specifically designed to avoid the problem of postmortem extravasation (Angiofil™, Fumedica, Switzerland) [29]. This product was mixed with paraffin oil of low viscosity (at 20 °C relative density between 0.810 and 0.875, dynamic viscosity between 25 mPas and 80 mPas and refractive index between 1.462 and 1.472) with a 6 % ratio. In order to avoid a sedimentation phenomenon, the syringe was heavily shaken before proceeding with the injection. Due to the physical properties of the contrast agent mixed with low viscosity paraffin oil, the contrast medium was manually injected at ambient temperature.

Table 1
Study population. Data about the anonymised subject reference (ASR), Gestational age (GA), weight, height, cranial perimeter (CP), sex, postmortem interval (PMI) equivalent to the period between time of expulsion and PMCTA examination, and scoring. When a parameter was not assessable it was noted NA.

ASR	GA (days)	Weight (gr)	Height (cm)	CP (cm)	Sex	PMI (months)	Scoring arterial	Scoring veinous	Scoring total	Failures (F) Interpretable (I)	Fresh (V) Frozen (O) Fixed (X)
69/98	168	548.7	32	19.7	M	240	0	6	6	F	O
80/05	NA	868	38	25.5	F	168	0	0	0	F	X
F03/16	106	39.2	13.5	8.5	NA	NA	0	0	0	F	O
F07/16	146	268.4	26.1	16.3	M	23	0	14	14	F	O
F09/16	154	524.5	29.4	19.4	M	21	25	10	35	I	O
F10/16	140	192.8	21.5	14.7	M	20	23	14	37	I	O
F12/16	175	345,8	26.6	19.1	M	20	28	16	44	I	O
F16/16	112	58.4	14	9.7	M	15	2	0	2	F	O
F18/16	151	117.5	23.5	14.4	M	21	0	0	0	F	O
F06/17	149	271.5	26.5	16.7	F	10	3	10	13	F	O
F14/17	159	316.5	27	16.5	F	18	0	10	10	F	O
F15/17	143	371.9	27	17.4	M	8	23	15	38	I	O
F16/17	133	212.6	23.5	14.8	M	7	28	15	43	I	O
F01/18	142	249.3	24.7	15.9	F	1	27	13	40	I	O
F03/18	173	696	32.5	21	M	16	20	4	24	I	O
F05/18	115	80.9	15.3	10.9	M	0.33	23	13	36	I	O
F08/18	154	295	25.4	16.8	M	0.63	1	0	1	F	O
F09/18	154	397.5	29.2	19.3	F	0.63	25	13	38	I	O
F10/18	168	551.8	32	20.5	F	0.2	28	15	43	I	V
F20/18	123	126	19	12	M	42	13	16	29	I	O
36/18	196	1498.1	38.7	29	M	0.16	27	15	42	I	V
F01/19	114	101	18.9	11.8	M	1	0	1	1	F	O
F03/19	170	645	32.4	20.5	F	0.75	13	13	26	I	O
F07/19	175	777.8	33	22.9	F	0.3	28	13	41	I	V
F02/20	156	501	30	19	M	0.5	25	13	38	I	V
Mean	**149.00**	**402.21**	**26.39**	**17.29**		**26.44**	**14.48**	**9.56**	**24.04**		
STD	**23.06**	**325.02**	**6.75**	**4.79**		**56.74**	**12.19**	**6.08**	**17.14**		
Median	**152.50**	**316.50**	**25.60**	**16.80**		**9.00**	**20.00**	**13.00**	**29.00**		

Site and method of injection

A radiographer trained in postmortem imaging [34] was dedicated to this study. When the peripheral vascular access was possible, the injection was always made using the same catheterization device (24GA 0.75IN – 0.7 mm x 19 mm – BD Nexiva™ Diffusics™, Mississauga, Canada) of the arteries and the umbilical vein as described by Sarda-Quarello [35]. The insertion needles were removed in order not to damage the umbilical vessels and thus avoid injection artefacts. Thereafter, the catheter has been purged of any air bubbles. When catheterization of the umbilical veins was not possible, a direct intracardiac injection was performed under ultrasound guidance. For the arterial phase, a manual injection of 7 mL of the contrast mixture was performed to fill the entire arterial system. In order to avoid extravasation through the other umbilical artery, the umbilical cord was clamped with a tight flexible tie. For the venous phase, an injection of 15 mL was performed

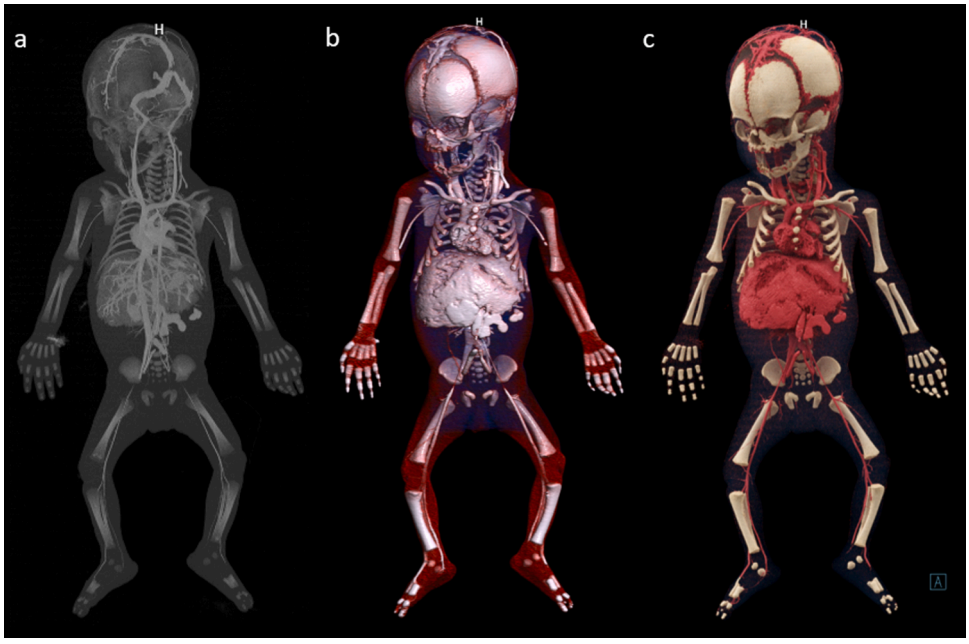

Fig. 1. Post-processing techniques: MIP - Maximal intensity projection (a) – VRT - Volume Rendering Technique (b) and CRT - Cinematic Rendering Technique (c) - anterior view.

to fill the entire venous system. The volume of contrast to be injected was determined empirically by injecting millilitre by millilitre until an optimal opacification of the vascular network was reached.

Image analysis

All MDCT acquisitions were transferred to a syngo.via workstation (Siemens™ Healthcare, Forchheim, Germany – version VB40B). Images were displayed using Maximal Intensity Projection (MIP), Volume Rendering (VRT) and Cinematic Rendering (CRT) Techniques (Siemens™) on different projections and orthogonal axes (coronal, sagittal and transversal) (Fig. 1). A radiographer, a board-certified forensic pathologist and a board-certified radiologist reviewed images in consensus. The following features were assessed during each review using MIP : (i) the vascular opacification (scored 0 when none, 1 when partial, 2 when complete (Fig. 2) both in the arterial phase and in the venous phase, (ii) the presence of imaging artefacts, and (iii) the overall quality of the radiological examination in taking into consideration the alteration state of the fetus, technique-related artefacts and filling of the vascular system (Table 1). A total opacification score (defined as the sum of the *per*-vessel opacification scores in a given subject) was also studied (Table 2). Noteworthy, this total vascular opacification covered the main body regions including the great vessels of the cervico-cerebral and thoraco-abdominal regions. The vascularity of the limbs was also examined but was not taken into account to assess the opacification (Table 3). An examination was considered as interpretable if the opacification was at least partial.

Statistical analysis

Measures of interest were reported in terms of mean values (median values when the data distributions were non-normal according to the Shapiro-Wilk test) with their associated 95 % Confidence Interval (CI). Frequency of each of the 3 levels of opacification was reported *per*-vessel compartment and *per* anatomical region. Difference of frequency of complete opacification between vascular compartments was studied using a two-sided Exact test. Correlation between foetus' weight and the *per*-vessel opacification score, between PMI and the total opacification score, and between the method of fetal preservation (coded on a ordinal scale as follows: formol = 0, frozen = 1, fresh = 2) and the total opacification score was investigated using Kendall's tau coefficient. Strength of correlation was interpreted as follows: tau $\geq$ 0.80, strong, 0.6 $\leq$ tau $<$ 0.80, moderate, 0.40 $\leq$ tau $<$ 0.60, weak and tau $<$ 0.40, poor. A p-value $<$ 0.05 was regarded as statistically significant for all tests cited above. The Statsdirect statistical software v3.3.5 was used for the analyses.

Results

Population

Clinical and morphological characteristics are given in Table 1.

Unenhanced imaging

Examples of unenhanced MDCT and post-contrast images are shown in Fig. 2. Unenhanced MDCT provided visualization of the fetal skeleton, but no differentiation of the soft tissues.

Procedure of injection

In two cases, the fetuses were too small, and the umbilical cord was mummified; thus, it was not feasible to inject the vessels. An intracardiac injection was performed under ultrasound guidance, but many artefacts appeared, such as filling of the pericardium, mainly resulting from heart slippage and its very small size (Fig. 3). In 23/25 (92 %) cases, an injection into the umbilical vessels was performed manually using flexible catheters (without the insertion needle).

Correlation between subject's characteristics and opacification score

Results are given in Table 4. A weak positive correlation between weight and opacification score was observed in 3 vessels only: iliac arteries (tau= 0.39, p= 0.0067), renal arteries (tau= 0.34, p= 0.0198), and descending aorta (tau= 0.32, p= 0.0293). A moderate negative correlation between PMI and total opacification score was observed (tau= -0.53, p= 0.0073). A moderate positive correlation was also observed between the method of fetal preservation and the total opacification score (tau= 0.49, p= 0.0007).

Opacification after the first injection

Even after a long postmortem interval causing an alteration of the fetus (Fig. 4a), after catheterizing an umbilical artery, the aorta was visible following the injection only 1mL of the mixture (Fig. 4b). After injection of 7mL, even microscopic arteries such as coronary arteries became visible (Fig. 5). In all succeeded cases, large vessels of the body were visible, such as the pulmonary arteries, the aorta, the renal arteries and the iliac arteries (Fig. 6a). The process also makes visible small vessels, such as the digital arteries of the upper and lower limbs (Fig. 6b). Additionally, vessels of the neck and the head, such as the polygon of Willis and the facial arteries and lingual arteries, were visible (Fig. 6c).

After the first injection phase, the arterial network appeared in 15/25 (60 %) subjects. In addition, it became visible in the limbs of 12/23 (52 %) fetuses.

Among the 10/25 (40 %) subjects considered as failures, 3/10 (30 %) fetuses still presented an interpretable opacification of large vessels such as the pulmonary arteries and the aortic arch. In these three failures, we observed an absence of accessibility to the vessels in the formalised fetus (Fig. 7a), a fragility of the vessels (due to postmortem alteration) and an abdominal extravasation of the contrast agent which no longer allowed the vascular analysis (Fig. 7b). Additionally, when the catheter was not properly purged, air bubbles appeared in the vessels, thereby reducing the opacification score.

Opacification after the second injection

By catheterizing the still ligated umbilical vein, an injection of 15 mL of the mixture was sufficient to opacify the entire venous system. After the second injection phase, the venous network appeared in 18/23 (78 %) subjects (Fig. 6d). Among the 7/25 (28 %) subjects considered as failures, 3 fetuses still presented interpretable opacification of the Arantius duct, jugular veins and the heart. Some injections were only interpretable in a single phase; 3 fetuses had an interpretable opacification score in venous injection, whereas arterial injection did not allow an interpretable opacification of the arterial network.

Proportions of subjects with a complete, partial and no opacification

Results are given in Table 1. For each anatomical region (head, trunk) we observed a complete opacification of the basilar trunk and the renal arteries in the arterial phase and the pulmonary veins in the venous phase in more than 14/23 (61 %) after injection.

Post processing of CT images

MIP reconstruction provided more details on the global opacification but only offered a 2D image (Fig. 1a). Volume Rendering Technique (VRT) offered a 3D image and allowed segmentation of bones and vessels in the different phases of acquisition (Fig. 1b). Cinematic Rendering Technique (CRT) provided additional information on the depth of the

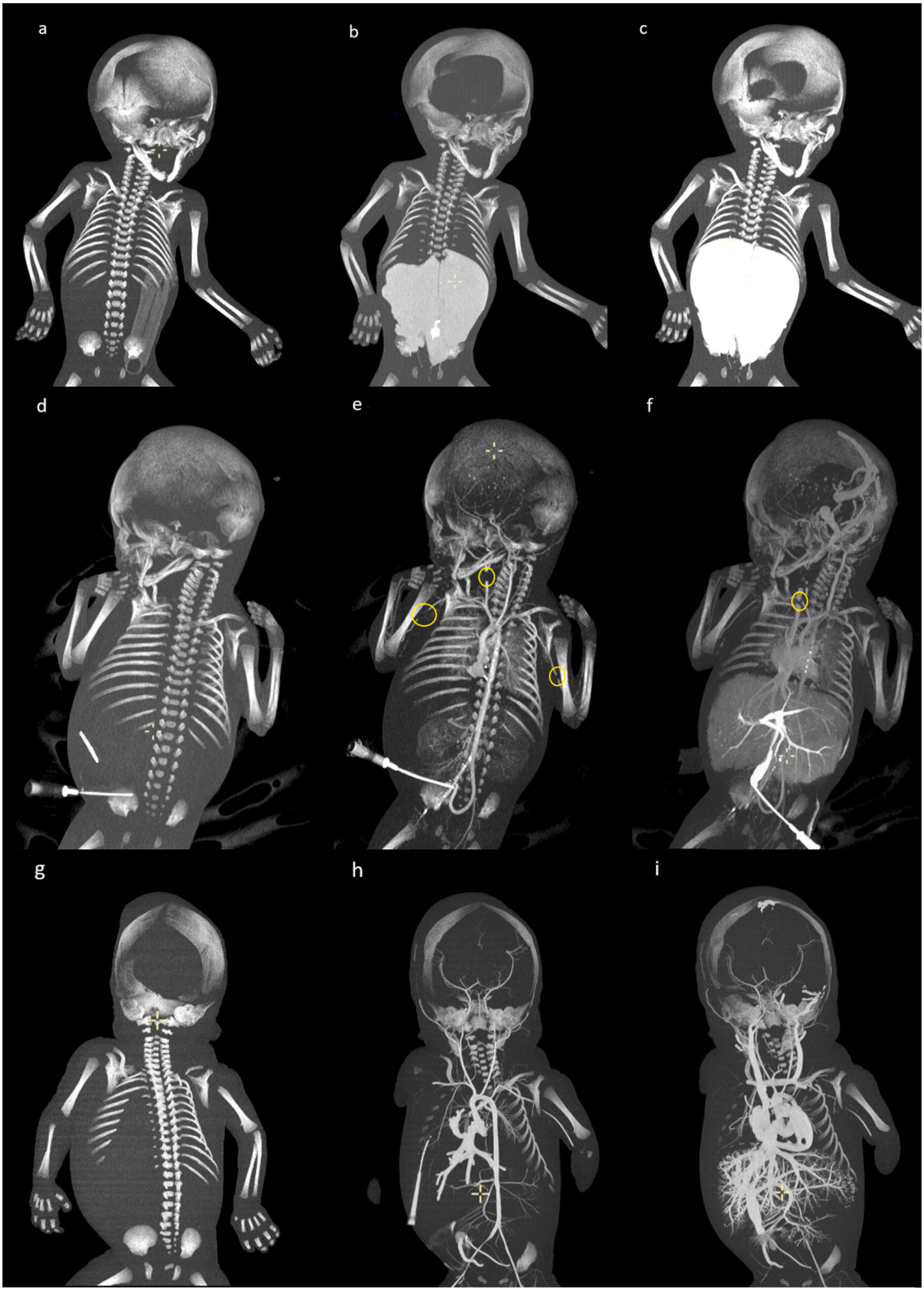

Fig. 2. *Fig. 2A (a-b-c)* Fetus deceased at 154 days of gestational age. CT angiography image using MIP before injection (a), after arterial opacification (b) and after venous opacification (c) show no opacification, corresponding to a score 0 and artefactual abdominal extravastion. *Fig. 2B (e-f-g)* Fetus deceased 170 days of gestational age. CT angiography image using MIP before injection (d), after arterial opacification (e) and after venous opacification (f) show no opacification (score 0), partial opacification (score 1 – yellow circle) and complete opacification (score 2). The yellow circles surround the brachial arteries and the right carotid artery (e) as well as the right brachiocephalic trunk (f). *Fig. 2C (g-h-i):* Fetus deceased 196 days of gestational age. CT angiography image using MIP before injection (g), after arterial opacification (h) and after venous opacification (i) show complete opacification (score 2) of the Willis polygon and hepatic veins.

Table 2
Proportions of subjects with a complete, partial and no opacification after the second injection of CA. Proportions are sorted *per*-vessel.

Complete opacification		Partial opacification		No opacification	
% of patients	Vessel	% of patients	Vessel	% of patients	Vessel
56	basilar trunk	20	anterior cerebral artery	48	posterior cerebral artery
48	middle cerebral artery	16	posterior cerebral artery	44	basilar trunk
40	anterior cerebral artery	12	middle cerebral artery	40	anterior cerebral artery
36	posterior cerebral artery	0	basilar trunk	40	middle cerebral artery
40	superior longitudinal sinus	12	cerebral veins	48	cerebral veins
52	renal artery	16	renal artery	64	aortic arch
48	superior mesenteric artery	16	pulmonary artery	56	descending aorta
40	descending aorta	8	iliac artery	52	pulmonary artery
40	iliac artery	8	aortic arch	52	iliac artery
32	pulmonary artery	4	descending aorta	48	superior mesenteric artery
28	aortic arch	4	superior mesenteric artery	32	renal artery
52	pulmonary vein	44	heart	68	arantius
32	hepatic veins	8	arantius	68	inferior veina cava
28	inferior veina cava	8	hepatic veins	68	renal veins
28	renal veins	4	pulmonary vein	60	hepatic veins
24	heart	4	inferior veina cava	44	pulmonary vein
24	arantius	4	renal veins	32	heart

tissue and preserved the details of the MIP reconstruction (Fig. 1c).

Discussion

The first results of this study is that MDCT protocol with an intra umbilical injection of a lipophilic contrast agent mixed with paraffin oil allowed the vascular opacification of the fetal vasculature. The opacification of the large vessels of the trunk and head made it possible to obtain an interpretable radiological image in the majority of cases studied (15/23 – 65 %). Most cases showed interpretable opacification of the large vessels after one of the two injections even though the limbs were not, or partially, opacified (9/15). In view of these findings, it was decided that the opacification of the trunk and the cephalic extremity were sufficient to consider that the opacification was interpretable. Analysis of the vascular opacification of the limbs should be considered in future studies.

The second result is that the limitations in time for fetal postmortem CT angiography described in the literature [32] can be compensated for by the use of an oily contrast product, and the technique can therefore be applied in the event of a post-mortem delay of more than 48 hours. This procedure with oily contrast agent was already described for the post-mortem CT angiography of preterm neonate [36] and newborns [37].

The study showed that arterial and venous opacification of the fetal vascular network is achievable by injecting a mixture of 6 % Angiofil^{TM} contrast medium with low viscosity paraffin oil by umbilical vascular access. The arterial injection of 7 ml then the injection of 15ml into the vein was sufficient for the complete opacification of the vascular network. The injection in the venous phase allowed an increase of the opacification score of the vessels, especially at the cardiac and hepatic

Table 3
Descriptive table of the vascular elements studied in the various anatomical sectors in order to judge the vascular opacification quality. Each anatomical segment reviewed was evaluated by an individual score of 0 (no opacification) - 1 (partial opacification) - 2 (complete opacification). The vascularity of the limbs was also examined but was not taken into account to assess the overall quality opacification. The results are shown in Table 1. All vessels analysed are abbreviated in brackets and included in the supplementary material.

Region	Arteries	Veins
Cervico-cerebral	Anterior cerebral artery (aca)	Superior longitudinal sinus (sls)
	Middle cerebral artery (mca)	Jugular veins (jv)
	Posterior cerebral artery (pca)	
	Basilar trunk (bt)	
	External carotid artery (eca)	
	Internal carotid artery (ica)	
	Vertebral arteries (va)	
	Common carotid arteries (cca)	
Thoracic, abdominal and pelvic	Aortic arch (aa)	Pulmonary arteries (pa)
	Descending aorta (da)	Heart
	Pulmonary veins (pv)	Inferior vena cava (ivc)
	Superior mesenteric artery (sma)	Hepatic veins (hv)
	Renal arteries (ra)	Renal veins (rv)
	Common iliac arteries (cia)	Arantius ductus (ad)
Upper limbs	Brachial arteries (ba)	Axillary vein (av)
	Radial/ulnar arteries (rda/ua)	Basilic/cubital vein
	Palmar arches (pas)	Palmar arch (pa)
Lower limbs	Femoral arteries (fa)	Femoral vein (fv)
	Tibial arteries (ta)	Tibial veins (tv)
	Plantar arches (plas)	Plantar arch (pla)

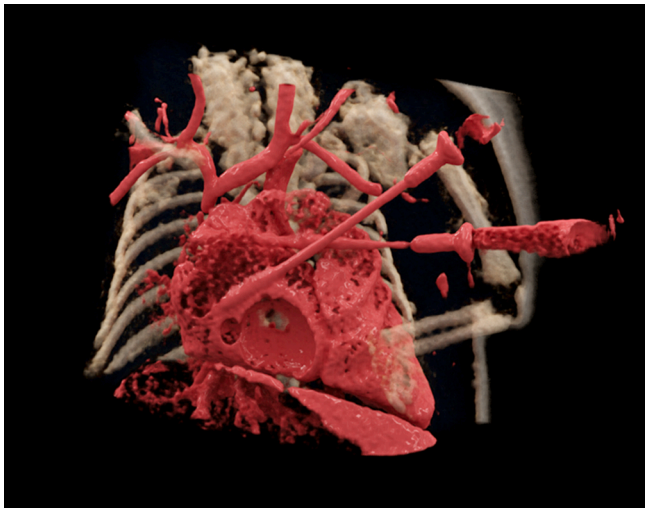

Fig. 3. PMCTA of a deceased fetus at 112 days of gestational age. Injection performed in the cardiac chambers under ultrasound guidance. CT angiography image in the anterior view using Cinematic Rendering Technique (CRT) highlight the visualisation of the heart and large vessels but extravasation of the contrast product is also observed. The needles used for the injection are still in place.

Table 4
Correlation between subject's weight and opacification score (a) and postmortem interval and arterial opacification (b).

(A) Vessel	*p*-value	tau
Iliac artery	0.0067	0.39 [0.05; 0.63]
Renal artery	0.0198	0.34 [-0.04; 0.58]
Descending aorta	0.0293	0.32 [-0.06; 0.59]
Anterior cerebral artery	0.0630	-
Middle cerebral artery	0.1304	-
Superior mesenteric artery	0.1424	-
Basilar trunk	0.1814	-
Posterior cerebral artery	0.2801	-
Aortic arch	0.3185	-
Pulmonary artery	0.3922	-
Total artery	0.1411	-

(B) Postmortem interval in months	p-value	tau
9.00 [0.72 ;20.0]	0.0055	-0.40 [-0.61; -0.08]

Kendall's tau is reported only when the correlation is significantly different from 0
Significance level $p < 0.05$
95 %CI is given into brackets

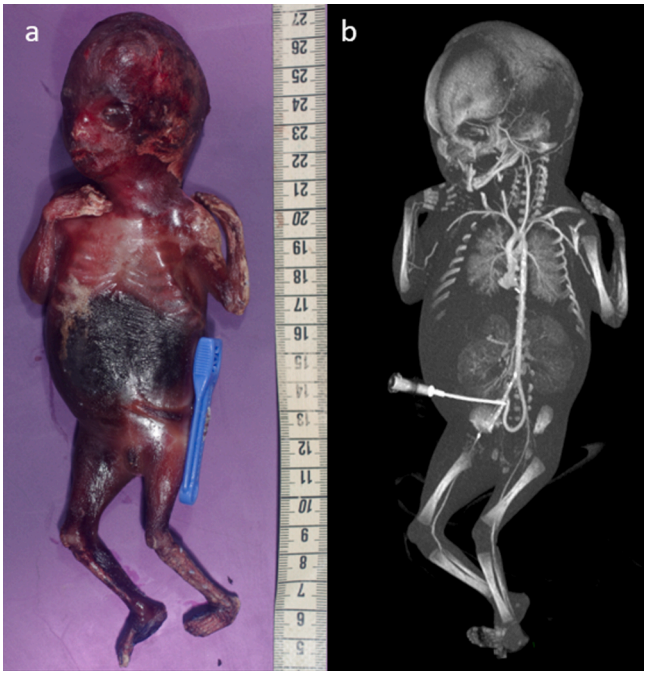

Fig. 4. Fetus deceased at 146 days of gestational age. The postmortem interval between expulsion and examination is 23 months. The stage of postmortem alteration is advanced (a), however CT angiography image in anterior view using Maximal Intensity Projection (MIP) after arterial opacification consecutive to the injection of 1 mL already demonstrates a good opacification of great vessels (b).

level. Nevertheless intravenous injection could not be carried out alone given that the arterial network was then not highlighted. The liver vessels were filled via the ductus Arantius - Ductus Venosus, connecting the umbilical vein to the terminal part of the inferior vena cava. This venous conduct allows some of the oxygenated blood to pass from the placenta through the umbilical vein to go almost directly into the right atrium of the fetal heart without passing through the liver. The Arantius canal stops functioning a few minutes after birth. It will spontaneously close again during the first week of life and remain in the form of a residue: the venous ligament of the liver. The venous phase allowed, through the ductus Arantius, an interpretable opacification of the heart

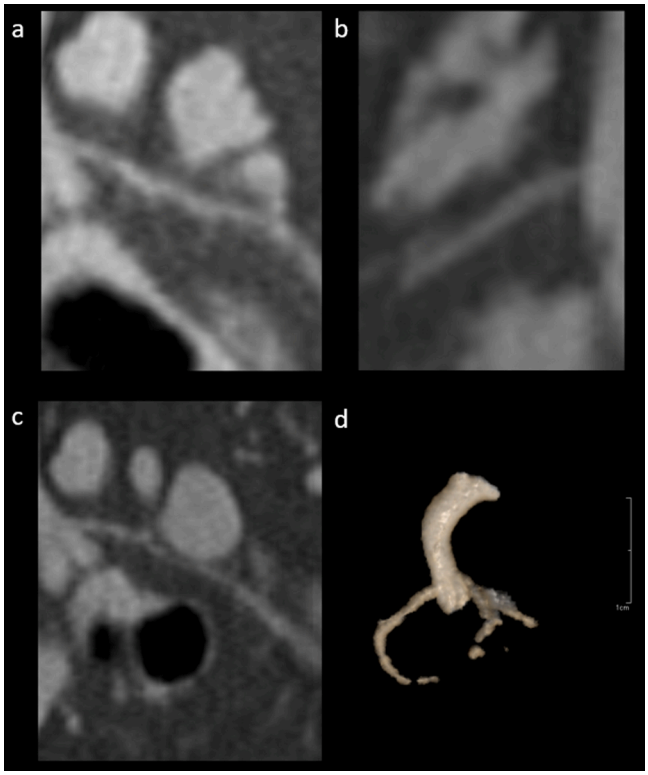

Fig. 5. Fetus deceased at 175 days of gestational age. The post-mortem interval between the expulsion and the examination is 20 months. CT angiography image using MIP after arterial opacification shows very small caliber arteries such as left anterior descending artery (a), right coronary artery (b) and circumflex artery (c). The CT angiography image using the Cinematic Rendering Technique (CRT) makes it possible to visualize the sinuses of Valsalva as well as the coronary arteries (d).

chambers by opacifying more particularly the right chambers of the heart.

Concerning the post-processing techniques used to assess CT images, MIP reconstruction allowed rapid assessment of vascularity and completeness of the vascular network and the scoring of opacification. The high dynamic range lighting of CRT ensured that the natural illumination of the rendered data generated a more realistic and visually attractive 3D image, which affects and improves the perception of depth and shape. In this way, the method provided anatomy models of the fetus and, therefore, improved predictive power [38,39].

The two-phase intra-umbilical injection method developed in this study allows visualizing the main vascular trunks, which may help pathologists to diagnose cardiovascular malformations. Further studies linked to autopsy findings should make it possible to assess the extent to which diagnosis is facilitated.

Our protocol resulted in umbilical injection failures in 40 % of cases. These failures were due to the small size of some fetuses (2/25) requiring a cardiac injection. Even without taking into account the risk of artefacts, the intracardiac injection was a difficult technique due to the location of the heart even when performed under ultrasound guidance. Other failures (8/25) were due to an inadequate method of preservation (freezing or formalin). We therefore recommend performing this examination on fetuses that have not undergone prolonged postmortem storage.

Imaging artefacts, already described in the literature [25], were observed, such as the sedimentation of the contrast product with paraffin oil, layering in the lumen of arterial system, and the incomplete opacification of certain veins.

The main limitation of our study was the limited sample size, which was due to the lack of donations to the department of anatomy. Since

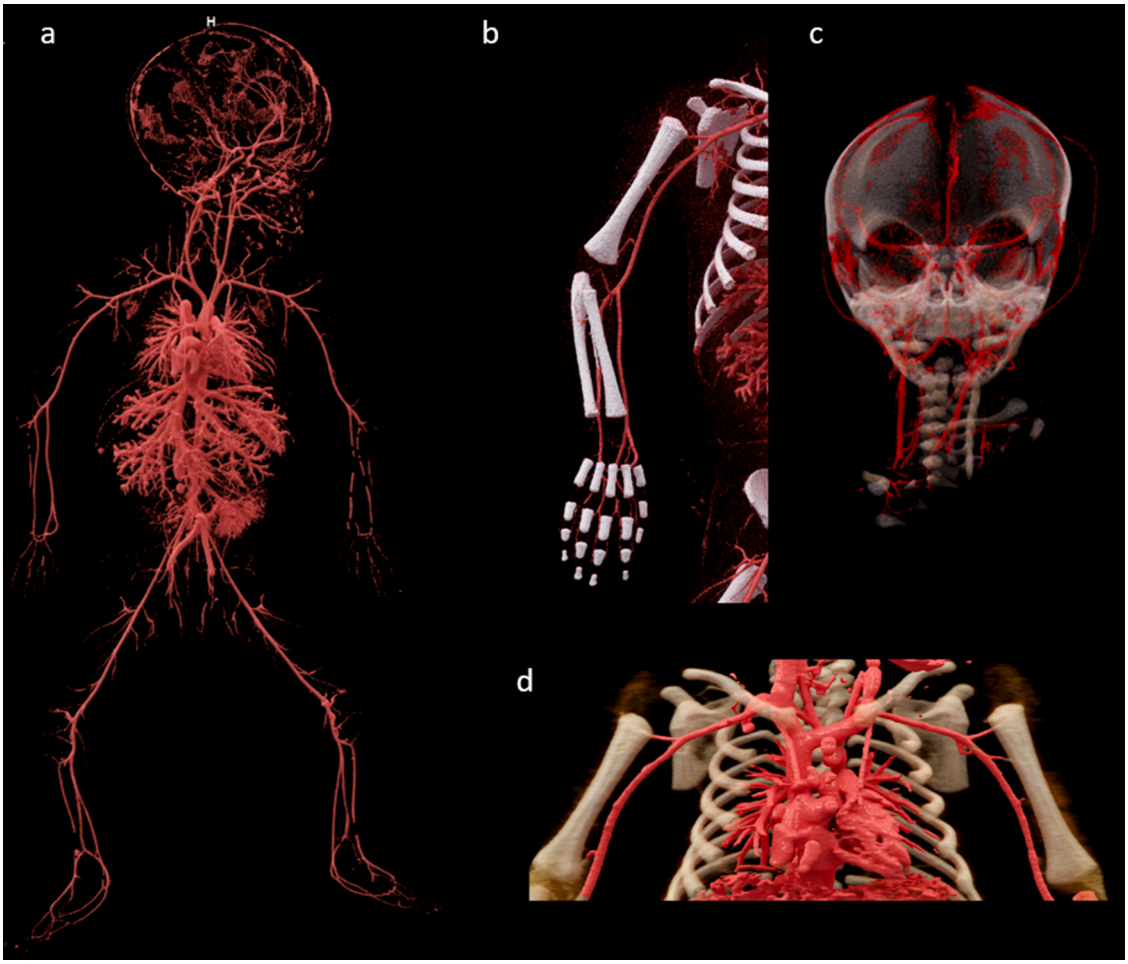

Fig. 6. Fetus deceased at 175 days of gestational age. CT angiography image after injection of 7mL in the arterial system shows opacification of the entire arterial system using Cinematic Rendering Technique (CRT) (a) highlighting small arteries such as digital arteries (b) Willis circle (c) in anterior view. Venous opacification after injection of 15 mL optimizes cardiac chambers opacification (d).

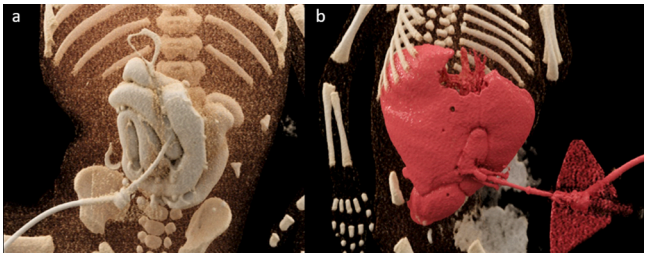

Fig. 7. Example of failures: CT angiography image using the Cinematic Rendering Technique (CRT) showing bowel injection in formalized fetus (A) and abdominal extravasation (B).

many fetuses were donated to the anatomy department after autopsy, radiological examination with injection of a contrast agent was therefore not feasible. Methodological limitations were also encountered. The fetuses studied were mostly frozen before examination and therefore did not represent an appropriate population.

Other future goals are the accurate mapping of abnormalities, which could be obtained by a systematization of the radiological reading. It has been shown that the development of adjacent brain structures and the appearance of the gyris induce changes in the position, path and relationship of brain arteries [40]. It is also necessary to study and establish an accurate mapping of the intrahepatic portal venous system to optimize the prenatal counselling and postnatal care due to fetal abnormalities of the umbilical-portal-systemic venous shunts [41]. Likewise, it will be essential to analyse the placenta with the same method to help figure out more causes of death due to placental causes such as abruption, fetal-maternal haemorrhage, cord accident, etc... [42].

Conclusion

PMCTA of the fetus is possible by manually injecting a lipophilic contrast agent mixed with paraffin oil into the umbilical vessels. The procedure takes place in two phases and requires a first intra-arterial injection and then a second intravenous injection. The technique allows visualization of the fetal vascular network, even after long post-mortem intervals. By providing detailed vascular images and contributing to a more comprehensive understanding of fetal vascular abnormalities, PMCTA could significantly advance medical knowledge and improve clinical practice in the field of fetal medicine. With continued further research and development, PMCTA may become an invaluable tool in the diagnostic and counselling process for affected families, offering hope for improved outcomes and a better understanding of fetal vascular pathologies.

Supplementary material captions

Appendix: anatomical diagram of the arteries (a) and veins (b) analyzed during the procedure, abbreviated according to table 3.

CRediT authorship contribution statement

Jessica Vanhaebost: Writing – review & editing, Writing – original draft, Methodology, Investigation, Formal analysis, Data curation, Conceptualization. **Nicolas Michoux:** Writing – review & editing, Software, Formal analysis. **Xavier de Spiegeleire:** Visualization, Methodology, Investigation, Formal analysis, Conceptualization. **Silke Grabherr:** Writing – review & editing, Validation, Supervision. **Emmanuel Coche:** Writing – review & editing, Visualization, Validation, Supervision, Resources.

Declaration of competing interest

The authors declare that they have no known competing financial interests or personal relationships that could have appeared to influence the work reported in this paper.

Acknowledgements

The authors would like to express their sincere gratitude to Catherine Behets professor of anatomy at UCLouvain and responsible for body donation for providing access to the fetuses studied in this research. Her contribution has been invaluable in facilitating the data collection process and enabling the analysis conducted in this study.

Supplementary materials

Supplementary material associated with this article can be found, in the online version, at doi:10.1016/j.fri.2024.200593.

References

[1] R.P. Kapur, Practicing pediatric pathology without a microscope, Mod. Pathol. 14 (3) (2001) 229–235, https://doi.org/10.1038/modpathol.3880290.
[2] C. Nezelof, T.A. Seemayer, J.A. Bridge, Contributions of pediatrics and pediatric pathology to the body of knowledge regarding human disease, Hum. Pathol. 41 (3) (2010) 309–315, https://doi.org/10.1016/j.humpath.2009.06.017.
[3] C. Wright, R.E. Lee, Investigating perinatal death: a review of the options when autopsy consent is refused, Arch. Dis. Child Fetal. Neonatal. Ed. 89 (4) (2004) F285–F288, https://doi.org/10.1136/adc.2003.022483.
[4] J.C. Hutchinson, X. Kang, S.C. Shelmerdine, V. Segers, C.M. Lombardi, M. M. Cannie, N.J. Sebire, J.C. Jani, O.J. Arthurs, Postmortem microfocus computed tomography for early gestation fetuses: a validation study against conventional autopsy, Am. J. Obstet. Gynecol. 218 (4) (2018), https://doi.org/10.1016/j.ajog.2018.01.040, 445.e441-445.e412.
[5] N.T. Griscom, S.G. Driscoll, Radiography of stillborn fetuses and infants dying at birth, AJR Am. J. Roentgenol. 134 (3) (1980) 485–489, https://doi.org/10.2214/ajr.134.3.485.
[6] O.E. ØE, E. A, H. Maartmann-Moe, R.S. Lachman, K. Rosendahl, Diagnostic value of radiography in cases of perinatal death: a population based study, Arch. Dis. Childhood Fetal Neonatal Edition 88 (6) (2003) F521–F524, https://doi.org/10.1136/fn.88.6.f521.
[7] O.E. Olsen, Radiography following perinatal death: a review, Acta Radiol. 47 (1) (2006) 91–99, https://doi.org/10.1080/02841850500406811.
[8] O.J. Arthurs, A.D. Calder, L. Kiho, A.M. Taylor, N.J. Sebire, Routine perinatal and paediatric post-mortem radiography: detection rates and implications for practice, Pediatr. Radiol. 44 (3) (2014) 252–257, https://doi.org/10.1007/s00247-013-2804-0.
[9] O.J. Arthurs, A.D. Calder, W.M. Klein, Is there still a role for fetal and perinatal post-mortem radiography? J. Forensic Radiol. Imaging 3 (1) (2015) 5–11, https://doi.org/10.1016/j.jofri.2014.12.004.
[10] X. Kang, A. Carlin, M.M. Cannie, T.C. Sanchez, J.C. Jani, Fetal postmortem imaging: an overview of current techniques and future perspectives, Am. J. Obstet. Gynecol. 223 (4) (2020) 493–515, https://doi.org/10.1016/j.ajog.2020.04.034.
[11] S. Grabherr, J. Grimm, P. Baumann, P. Mangin, Application of contrast media in post-mortem imaging (CT and MRI), Radiol. Med. 120 (9) (2015) 824–834, https://doi.org/10.1007/s11547-015-0532-2.
[12] M. Vaneckova, Z. Seidl, B. Goldova, I. Vitkova, A. Baxova, P. Petrovicky, V. Sebron, P. Calda, Post-mortem magnetic resonance imaging and its irreplaceable role in determining CNS malformation (hydranencephaly)–case report, Brain Dev. 32 (5) (2010) 417–420, https://doi.org/10.1016/j.braindev.2009.03.011.
[13] S. Addison, O.J. Arthurs, S. Thayyil, Post-mortem MRI as an alternative to non-forensic autopsy in foetuses and children: from research into clinical practice, Br. J. Radiol. 87 (1036) (2014) 20130621, https://doi.org/10.1259/bjr.20130621.
[14] E. Widjaja, E.H. Whitby, M. Cohen, M.N. Paley, P.D. Griffiths, Post-mortem MRI of the foetal spine and spinal cord, Clin. Radiol. 61 (8) (2006) 679–685, https://doi.org/10.1016/j.crad.2006.01.016.
[15] S. Thayyil, N.J. Sebire, L.S. Chitty, A. Wade, W. Chong, O. Olsen, R.S. Gunny, A. C. Offiah, C.M. Owens, D.E. Saunders, R.J. Scott, R. Jones, W. Norman, S. Addison, A. Bainbridge, E.B. Cady, E.D. Vita, N.J. Robertson, A.M. Taylor, Post-mortem MRI versus conventional autopsy in fetuses and children: a prospective validation study, Lancet 382 (9888) (2013) 223–233, https://doi.org/10.1016/s0140-6736(13)60134-8.
[16] S. Thayyil, J.O. Cleary, N.J. Sebire, R.J. Scott, K. Chong, R. Gunny, C.M. Owens, O. E. Olsen, A.C. Offiah, H.G. Parks, L.S. Chitty, A.N. Price, T.A. Yousry, N. J. Robertson, M.F. Lythgoe, A.M. Taylor, Post-mortem examination of human fetuses: a comparison of whole-body high-field MRI at 9.4 T with conventional MRI and invasive autopsy, Lancet 374 (9688) (2009) 467–475, https://doi.org/10.1016/s0140-6736(09)60913-2.
[17] F.P. Cafarelli, G. Grilli, G. Zizzo, G. Bertozzi, N. Giuliani, P. Mahakkanukrauh, A. Pinto, G. Guglielmi, Postmortem imaging: an update, Semin. Ultrasound CT MR 40 (1) (2019) 86–93, https://doi.org/10.1053/j.sult.2018.10.012.
[18] P. Krantz, S. Holtås, Postmortem computed tomography in a diving fatality, J. Comput. Assist. Tomogr. 7 (1) (1983) 132–134, https://doi.org/10.1097/00004728-198302000-00024.
[19] Y. Dawood, M.F.J. Buijtendijk, H. Shah, J.A. Smit, K. Jacobs, J. Hagoort, R.-J. Oostra, T. Bourne, M.J.B. van den Hoff, B.S. de Bakker, Imaging fetal anatomy, Seminars Cell Develop. Biol. 131 (2022) 78–92, https://doi.org/10.1016/j.semcdb.2022.02.023.
[20] C. Chevallier, F. Doenz, P. Vaucher, C. Palmiere, A. Dominguez, S. Binaghi, P. Mangin, S. Grabherr, Postmortem computed tomography angiography vs. conventional autopsy: advantages and inconveniences of each method, Int. J. Legal. Med. 127 (5) (2013) 981–989, https://doi.org/10.1007/s00414-012-0814-3.
[21] S. Grabherr, V. Djonov, K. Yen, M.J. Thali, R. Dirnhofer, Postmortem angiography: review of former and current methods, AJR Am. J. Roentgenol. 188 (3) (2007) 832–838, https://doi.org/10.2214/ajr.06.0787.
[22] F.R. Pluchinotta, P. Porayette, A.H. Zaidi, J. Baci, L. Teot, S.P. Sanders, S. P. Prabhu, Postmortem imaging in congenital heart disease: preliminary experience, Acta Radiol. 56 (10) (2015) 1264–1272, https://doi.org/10.1177/0284185114555047.
[23] S. Grabherr, F. Doenz, B. Steger, R. Dirnhofer, A. Dominguez, B. Sollberger, E. Gygax, E. Rizzo, C. Chevallier, R. Meuli, P. Mangin, Multi-phase post-mortem CT angiography: development of a standardized protocol, Int. J. Legal. Med. 125 (6) (2011) 791–802, https://doi.org/10.1007/s00414-010-0526-5.
[24] F.Z. Mokrane, F. Savall, L. Dercle, E. Crubezy, N. Telmon, H. Rousseau, F. Dedouit, Technical note: A preliminary comparative study between classical and interventional radiological approaches for multi-phase post-mortem CT angiography, Forensic Sci. Int. 271 (2017) 23–32, https://doi.org/10.1016/j.forsciint.2016.12.008.
[25] C. Bruguier, P.J. Mosimann, P. Vaucher, A. Uské, F. Doenz, C. Jackowski, P. Mangin, S. Grabherr, Multi-phase postmortem CT angiography: recognizing technique-related artefacts and pitfalls, Int. J. Legal. Med. 127 (3) (2013) 639–652, https://doi.org/10.1007/s00414-013-0840-9.
[26] S. Grabherr, C. Egger, R. Vilarino, L. Campana, M. Jotterand, F. Dedouit, Modern post-mortem imaging: an update on recent developments, Forensic Sci. Res. 2 (2) (2017) 52–64, https://doi.org/10.1080/20961790.2017.1330738.
[27] S. Ross, D. Spendlove, S. Bolliger, A. Christe, L. Oesterhelweg, S. Grabherr, M. J. Thali, E. Gygax, Postmortem whole-body CT angiography: evaluation of two contrast media solutions, AJR Am. J. Roentgenol. 190 (5) (2008) 1380–1389, https://doi.org/10.2214/ajr.07.3082.
[28] F.Z. Mokrane, L. Dercle, O. Meyrignac, É. Crubézy, H. Rousseau, N. Telmon, F. Dedouit, Towards multi-phase postmortem CT angiography in children: a study on a porcine model, Int. J. Legal. Med. 132 (5) (2018) 1391–1403, https://doi.org/10.1007/s00414-018-1783-y.
[29] S. Grabherr, M. Dominietto, L. Yu, V. Djonov, B. Müller, S. Friess, Angiofil: a novel radio-contrast agent for post-mortem micro-angiography, Opt. Eng. + Appl. SPIE 7078 (2008).
[30] S. Grabherr, V. Djonov, A. Friess, M.J. Thali, G. Ranner, P. Vock, R. Dirnhofer, Postmortem angiography after vascular perfusion with diesel oil and a lipophilic contrast agent, AJR Am. J. Roentgenol. 187 (5) (2006) W515–W523, https://doi.org/10.2214/ajr.05.1394.
[31] L. Sarda-Quarello, L. Tuchtan, J. Torrents, M.-D. Piercecchi-Marti, C. Bartoli, P.-E. Laurent, B. Bourlière-Najean, P. Petit, E. Quarello, G. Gorincour, Perinatal death: Is there a place for post-mortem angio-CT? J. Forensic Radiol. Imaging 3 (1) (2015) 1–4, https://doi.org/10.1016/j.jofri.2015.02.002.
[32] U.N. Tumanova, V.M. Lyapin, V.G. Bychenko, A.I. Shchegolev, G.T. Sukhikh, Postmortem computed tomography angiography of newborns, Bull. Exp. Biol. Med. 170 (2) (2020) 268–274, https://doi.org/10.1007/s10517-020-05049-4.
[33] S. Grabherr, E. Gygax, B. Sollberger, S. Ross, L. Oesterhelweg, S. Bolliger, A. Christe, V. Djonov, M.J. Thali, R. Dirnhofer, Two-step postmortem angiography with a modified heart-lung machine: preliminary results, AJR Am. J. Roentgenol. 190 (2) (2008) 345–351, https://doi.org/10.2214/ajr.07.2261.
[34] B. Schneider, C. Chevallier, A. Dominguez, C. Bruguier, C. Elandoy, P. Mangin, S. Grabherr, The forensic radiographer: a new member in the medicolegal team, Am. J. Forensic Med. Pathol. 33 (1) (2012) 30–36, https://doi.org/10.1097/PAF.0b013e31820c6aa3.
[35] L. Sarda-Quarello, C. Bartoli, P.E. Laurent, J. Torrents, M.D. Piercecchi-Marti, S. Sigaudy, D. Ariey-Bonnet, G. Gorincour, Whole body perinatal postmortem CT

angiography, Diagn. Interv. ImAging 97 (1) (2016) 121–124, https://doi.org/10.1016/j.diii.2014.11.002.
[36] C. Egger, F. Dédouit, B. Schrag, S. Hanquinet, T. Fracasso, A forensic case of hydranencephaly in a preterm neonate fully documented by postmortem imaging techniques, Forensic Sci. Res. 8 (1) (2023) 79–83, https://doi.org/10.1093/fsr/owad002.
[37] K.J. Woźniak, A. Moskała, P. Kluza, K. Romaszko, O. Lopatin, E. Rzepecka-Woźniak, Whole-body post-mortem computed tomography angiography of a newborn revealing transposition of great arteries, Int. J. Legal. Med. 129 (6) (2015) 1253–1258, https://doi.org/10.1007/s00414-015-1267-2.
[38] M.R. Bueno, C. Estrela, J.M. Granjeiro, M.R.A. Estrela, B.C. Azevedo, A. Diogenes, Cone-beam computed tomography cinematic rendering: clinical, teaching and research applications, Braz. Oral Res. 35 (2021) e024, https://doi.org/10.1590/1807-3107bor-2021.vol35.0024.
[39] P. Debevec, Rendering synthetic objects into real scenes: bridging traditional and image-based graphics with global illumination and high dynamic range photography, in: Paper presented at the Proceedings of the 25th annual conference on Computer graphics and interactive techniques, 1998.
[40] A. Kulenović, F. Dilberović, Changes in blood vessels in fetuses 4 to 9 months intrauterine life old by postmortem angiography method, Bosn. J. Basic Med. Sci. 4 (3) (2004) 50–54, https://doi.org/10.17305/bjbms.2004.3394.
[41] R. Achiron, Z. Kivilevitch, Fetal umbilical-portal-systemic venous shunt: in-utero classification and clinical significance, Ultrasound. Obstet. Gynecol. 47 (6) (2016) 739–747, https://doi.org/10.1002/uog.14906.
[42] U. Fatima, R. Sherwani, T. Khan, S. Zaheer, Foetal autopsy-categories and causes of death, J. Clin. Diagn. Res. 8 (10) (2014), https://doi.org/10.7860/jcdr/2014/9226.4920. Fc05-08.